

Noise-Calibrated Inference from Differentially Private Sufficient Statistics in Exponential Families

Amir Asiaee¹

Samhita Pal¹

¹Department of Biostatistics, Vanderbilt University Medical Center, Nashville, TN, USA
{amir.asiaeetaheri, samhita.pal}@vumc.org

Abstract

Many differentially private (DP) data release systems either output DP synthetic data and leave analysts to perform inference as usual, which can lead to severe miscalibration, or output a DP point estimate without a principled way to do uncertainty quantification. This paper develops a clean and tractable middle ground for exponential families: release only DP sufficient statistics, then perform noise-calibrated likelihood-based inference and optional parametric synthetic data generation as post-processing. Our contributions are: (1) a general recipe for approximate-DP release of clipped sufficient statistics under the Gaussian mechanism; (2) asymptotic normality, explicit variance inflation, and valid Wald-style confidence intervals for the plug-in DP MLE; (3) a noise-aware likelihood correction that is first-order equivalent to the plug-in but supports bootstrap-based intervals; and (4) a matching minimax lower bound showing the privacy distortion rate is unavoidable. The resulting theory yields concrete design rules and a practical pipeline for releasing DP synthetic data with principled uncertainty quantification, validated on three exponential families and real census data.

1 INTRODUCTION

Synthetic data is often promoted as a privacy-friendly alternative to sharing raw datasets. However, the *scientific* objective is rarely to obtain a dataset that merely “looks realistic”; it is to enable valid inference about population parameters (standard errors, p -values, coverage) and, increasingly, valid causal conclusions. Recent benchmarks show that many DP synthetic data methods preserve some low-dimensional marginals yet can fail badly for inferential validity and hypothesis testing when analysts treat the synthetic data as real [Tao et al., 2022, Räisä et al., 2023, Perez

et al., 2024]. These failures are not surprising: differential privacy injects randomness that must be accounted for in uncertainty quantification.

This paper focuses on the most mathematically tractable and widely used regime where *sufficient statistics exist*: regular exponential family models. In exponential families, likelihood-based inference depends on the dataset only through the empirical sufficient statistic $\bar{S} = n^{-1} \sum_i s(X_i)$. This creates a natural and clean separation between privacy and inference: (1) release a DP-noisy sufficient statistic \tilde{S} , then (2) perform noise-calibrated inference from \tilde{S} alone. Because any downstream computation—including parameter estimation, confidence intervals, and parametric synthetic data generation—is a deterministic function of the released statistic, it inherits the same DP guarantee by post-processing.

Although DP inference and DP synthetic data have each received attention [Ferrando et al., 2022, Bernstein and Sheldon, 2018, McKenna et al., 2021, 2022], few works provide a unified treatment that (a) gives explicit asymptotic theory for inference from DP sufficient statistics, (b) quantifies the exact variance inflation due to privacy, and (c) connects parametric synthetic data generation to the same inferential framework. We fill this gap for exponential families.

1.1 CONTRIBUTIONS AND PAPER ROADMAP

We formalize a pipeline:

$$D = \{X_i\}_{i=1}^n \longrightarrow \tilde{S} \longrightarrow \tilde{\theta} \quad (\longrightarrow D^{\text{syn}}).$$

- **DP mechanism:** release a noisy empirical sufficient statistic \tilde{S} using the Gaussian mechanism [Dwork et al., 2006, Dwork and Roth, 2014].
- **Inference:** compute either a plug-in DP MLE $\tilde{\theta}_{\text{plug}}$ or a noise-aware estimator $\tilde{\theta}_{\text{NA}}$.
- **Optional synthetic data:** sample $D^{\text{syn}} \sim p(\cdot | \tilde{\theta})$; by post-processing, the synthetic data inherits DP.

We provide (i) explicit asymptotic variance inflation, (ii)

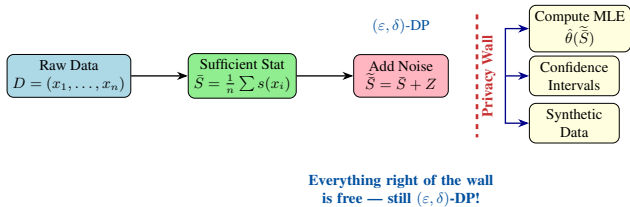


Figure 1: Pipeline overview. The noisy sufficient statistic \tilde{S} is the only DP-protected release; all downstream tasks inherit the same (ϵ, δ) -DP guarantee by post-processing.

valid confidence intervals, and (iii) a lower bound in a canonical subclass that matches the upper bound rate.

2 RELATED WORK

DP estimation and minimax rates. The foundational theory of DP estimation establishes that privacy imposes a cost on statistical accuracy. Dwork et al. [2006] introduced the Laplace and Gaussian mechanisms, calibrating noise to the sensitivity of a query. Early work connecting DP to classical statistical inference includes Wasserman and Zhou [2010]. For mean estimation of bounded data, Smith [2011] showed that (ϵ, δ) -DP estimators can achieve rates close to those of non-private estimators when n is large relative to $1/\epsilon$, while lower bounds due to Duchi et al. [2018] demonstrate that an $\Omega(1/(n\epsilon))$ RMSE distortion is unavoidable in the local DP model and also appears in the central model for sufficiently small ϵ . In the central model, Cai et al. [2021] established tight minimax rates for parameter estimation under (ϵ, δ) -DP, showing that the cost of privacy in ℓ_2 risk is $\Theta(d/(n^2\epsilon^2))$ for d -dimensional bounded problems; our Theorem 3 recovers the $d = 1$ case. For settings that rely heavily on Gaussian noise, alternative privacy accounting frameworks such as Gaussian differential privacy [Dong et al., 2022] provide a complementary perspective.

DP inference and confidence intervals. A central challenge is constructing valid confidence intervals when estimators are perturbed for privacy. General-purpose approaches include parametric bootstrap methods for DP confidence intervals [Ferrando et al., 2022] and DP hypothesis tests for linear regression [Alabi and Vadhan, 2022]. Finite-sample DP confidence intervals for the Gaussian mean were studied by Karwa and Vadhan [2018]. Asymptotic inference for DP M-estimators via noisy optimization was developed by Avella-Medina et al. [2023]. Simulation-based, finite-sample inference procedures for privatized data were studied by Awan and Wang [2025]. Noise-aware Bayesian inference for exponential families that accounts for DP noise in sufficient statistics was developed by Bernstein and Sheldon [2018], who showed how to incorporate the known noise distribution into a conjugate posterior update. More recently, Wang et al. [2025] developed a general DP bootstrap framework with privacy-aware variance estimation, and Covington et al. [2025] provided unbiased DP estimators with valid confidence intervals for a broad class of statistical function-

als. Awan and Slavković [2018] studied DP inference for the binomial proportion and related one-parameter families via optimal noise mechanisms that achieve exact finite-sample inference. In graph exponential-family models, Karwa and Slavković [2016] studied inference from DP-noisy sufficient statistics (noisy degrees) and synthetic graph generation.

DP synthetic data generation. Large-scale empirical benchmarks show that marginal-based / workload-based methods can outperform GAN-based methods for tabular synthesis, but inferential validity is not automatic [Tao et al., 2022]. State-of-the-art synthesis frameworks include Private-PGM and its MST/NIST-MST instantiations [McKenna et al., 2021], the workload-adaptive AIM mechanism [McKenna et al., 2022], and more recent approaches that incorporate geometry-aware losses and optimal transport [Donhauser et al., 2024]. A complementary line studies how to *analyze* DP synthetic data with correct uncertainty, including noise-aware synthetic data generation plus multiple imputation [Räisä et al., 2023] and empirical studies warning about inflated type-I error when synthetic data are analyzed naively [Perez et al., 2024].

Positioning. Our work is closest in spirit to Bernstein and Sheldon [2018] but differs in two ways. First, we provide a complete frequentist asymptotic theory—including explicit variance inflation formulas, Wald confidence intervals, and a matching lower bound—that complements their Bayesian treatment. Second, we show how the same released DP sufficient statistic can serve dual purposes: frequentist inference and parametric synthetic data generation, with both inheriting the same privacy guarantee. This unifies the “DP inference” and “DP synthetic data” literatures in the exponential-family setting. We note that the individual theoretical components—delta-method CLT for DP estimators and Le Cam lower bounds—are well known in the DP statistics literature; our contribution is their integration into a single, practical pipeline with thorough empirical validation and a clear demonstration that naive synthetic-data analysis fails.

3 SETUP

3.1 EXPONENTIAL FAMILY MODELS

Let $X \in \mathcal{X}$ and consider a (minimal) regular exponential family with natural parameter $\theta \in \Theta \subset \mathbb{R}^d$:

$$p_\theta(x) = h(x) \exp(\langle \theta, s(x) \rangle - A(\theta)), \quad (1)$$

where $s(x) \in \mathbb{R}^d$ is the sufficient statistic and $A(\theta)$ is the log-partition function. Given i.i.d. data $D = \{X_i\}_{i=1}^n$, the empirical sufficient statistic is

$$\bar{S}(D) = \frac{1}{n} \sum_{i=1}^n s(X_i) \in \mathbb{R}^d.$$

The (non-private) maximum likelihood estimator (MLE) $\hat{\theta}$ satisfies $\nabla A(\hat{\theta}) = \bar{S}(D)$ when the MLE exists.

Algorithm 1 DP Sufficient Statistic Release and Inference (Exponential Families)

- Require:** Dataset $D = \{X_i\}_{i=1}^n$, bound B , privacy (ε, δ)
- 1: Compute $\bar{S} = \frac{1}{n} \sum_{i=1}^n s(X_i)$ \triangleright sufficient statistic
 - 2: Set $\Delta_2 \leftarrow 2B/n$ $\triangleright \ell_2$ sensitivity of \bar{S}
 - 3: Set $\sigma \leftarrow \text{AGM}(\Delta_2, \varepsilon, \delta)$ \triangleright analytic Gaussian calibration [Balle and Wang, 2018]
 - 4: Sample $Z \sim \mathcal{N}(0, \sigma^2 I_d)$ and release $\tilde{S} = \bar{S} + Z$
 - 5: **Plug-in:** $\tilde{\theta}_{\text{plug}} \leftarrow (\nabla A)^{-1}(\tilde{S})$
 - 6: **Noise-aware:** $\tilde{\theta}_{\text{NA}} \leftarrow \arg \max_{\theta \in \Theta} \log p(\tilde{S} | \theta)$ (Section 4.3)
 - 7: (Optional) Sample synthetic data $D^{\text{syn}} \sim p(\cdot | \tilde{\theta}_{\text{plug}})$ (or $\tilde{\theta}_{\text{NA}}$)
-

3.2 DIFFERENTIAL PRIVACY AND THE GAUSSIAN MECHANISM

Two datasets D, D' are *neighbors* if they differ in a single record. A randomized mechanism \mathcal{M} is (ε, δ) -DP if for all neighboring D, D' and measurable sets E ,

$$\Pr(\mathcal{M}(D) \in E) \leq e^\varepsilon \Pr(\mathcal{M}(D') \in E) + \delta.$$

We use the Gaussian mechanism [Dwork et al., 2006, Dwork and Roth, 2014].

Assumption 1 (Bounded sufficient statistics). There exists $B > 0$ such that $\|s(x)\|_2 \leq B$ for all $x \in \mathcal{X}$.

Under Assumption 1, the ℓ_2 sensitivity of $\bar{S}(D)$ is at most $\Delta_2 = 2B/n$.

4 MECHANISMS AND ESTIMATORS

4.1 DP SUFFICIENT STATISTIC RELEASE

Here $\text{AGM}(\Delta_2, \varepsilon, \delta)$ denotes the analytic Gaussian mechanism calibration that returns the smallest σ such that adding $Z \sim \mathcal{N}(0, \sigma^2 I_d)$ to a query with ℓ_2 sensitivity Δ_2 is (ε, δ) -DP [Balle and Wang, 2018]. Throughout, we set $\delta = 1/n^2$ for all experiments; the analytic Gaussian mechanism calibration [Balle and Wang, 2018] then determines the minimal σ .

Theorem 1 (Privacy of sufficient-statistic release). *Under Assumption 1, releasing $\tilde{S} = \bar{S}(D) + Z$ with $Z \sim \mathcal{N}(0, \sigma^2 I_d)$ and σ as in Algorithm 1 is (ε, δ) -DP. Moreover, any (randomized) post-processing of \tilde{S} (including $\tilde{\theta}$ and D^{syn}) is also (ε, δ) -DP.*

Proof sketch. The ℓ_2 sensitivity of \bar{S} is at most $2B/n$. The stated σ is chosen by the analytic Gaussian mechanism calibration, which gives an (ε, δ) -DP guarantee for the Gaussian mechanism for any $\varepsilon > 0$ [Balle and Wang, 2018]; DP then follows from the Gaussian mechanism guarantee and post-processing invariance [Dwork et al., 2006, Dwork and Roth, 2014]. \square

4.2 PLUG-IN DP MLE AND ASYMPTOTIC NORMALITY

The plug-in estimator solves $\nabla A(\tilde{\theta}_{\text{plug}}) = \tilde{S}$. In a regular exponential family, $\nabla^2 A(\theta) = I(\theta)$ equals the Fisher information for one sample.

Assumption 2 (Regularity). The model is a minimal regular exponential family with θ_0 in the interior of Θ . The Fisher information $I(\theta_0)$ is positive definite.

Theorem 2 (Asymptotic distribution and variance inflation). *Under Assumptions 1–2, the plug-in DP MLE satisfies*

$$\sqrt{n} (\tilde{\theta}_{\text{plug}} - \theta_0) \xrightarrow{d} \mathcal{N}(0, I(\theta_0)^{-1} + n\sigma^2 I(\theta_0)^{-2}),$$

where σ^2 is the variance of the Gaussian noise in Algorithm 1 and $I(\theta_0)^{-2} := I(\theta_0)^{-1} I(\theta_0)^{-1}$. Equivalently,

$$\tilde{\theta}_{\text{plug}} - \theta_0 = \underbrace{O_p(n^{-1/2})}_{\text{sampling}} + \underbrace{O_p(\sigma)}_{\text{privacy}}.$$

When σ is calibrated for (ε, δ) -DP with ℓ_2 sensitivity $\Delta_2 = 2B/n$, the noise scale is proportional to Δ_2 and decreases with ε (up to $\log(1/\delta)$ factors), yielding the familiar $O_p((n\varepsilon)^{-1})$ privacy distortion rate for bounded problems.

Proof sketch. The proof decomposes the error into a sampling term and a privacy term that are independent. (i) The multivariate central limit theorem (CLT) gives $\sqrt{n}(\bar{S} - \mu(\theta_0)) \xrightarrow{d} \mathcal{N}(0, I(\theta_0))$, and the delta method applied through the inverse mean-parameter map $(\nabla A)^{-1}$ yields the classical $I(\theta_0)^{-1}/n$ variance. (ii) A first-order Taylor expansion of $(\nabla A)^{-1}$ around \tilde{S} gives $\tilde{\theta}_{\text{plug}} - \hat{\theta} = I(\hat{\theta})^{-1} Z + O_p(\|Z\|^2)$, contributing the $\sigma^2 I(\theta_0)^{-2}$ privacy variance. (iii) Since the Gaussian noise Z is independent of the data, the two variance components add. The full proof is in Appendix A. \square

Corollary 1 (When does privacy preserve classical efficiency?). *Under the conditions of Theorem 2, if $n\varepsilon^2 \rightarrow \infty$ (equivalently $\varepsilon \gg n^{-1/2}$ up to log factors in δ), then the privacy-induced variance vanishes and $\tilde{\theta}_{\text{plug}}$ is asymptotically as efficient as the non-private MLE. If $n\varepsilon^2$ is bounded, DP noise contributes a non-negligible variance inflation.*

4.3 NOISE-AWARE LIKELIHOOD CORRECTION

The plug-in estimator is first-order correct under smoothness, but in practice we often clip or otherwise sanitize $s(x)$ to bound sensitivity, inducing bias. Noise-aware inference explicitly models the DP noise and (optionally) the clipping.

A simple approach is to define the *noisy statistic likelihood*:

$$\ell_{\text{NA}}(\theta; \tilde{S}) := \log p(\tilde{S} | \theta), \quad (2)$$

where $p(\tilde{S} | \theta)$ is induced by the data model and the DP mechanism. In general, this is an intractable convolution, but it becomes tractable in two regimes:

- **CLT regime:** Approximate $\tilde{S} \mid \theta \approx \mathcal{N}(\nabla A(\theta), I(\theta)/n)$. Then $\tilde{\tilde{S}} \mid \theta \approx \mathcal{N}(\nabla A(\theta), I(\theta)/n + \sigma^2 I)$.
- **Conjugate / exact regimes:** For certain families and priors, exact noise-aware Bayes is available [Bernstein and Sheldon, 2018].

In the CLT regime, the noise-aware estimator solves a generalized least squares problem:

$$\tilde{\theta}_{\text{NA}} = \arg \min_{\theta \in \Theta} (\tilde{\tilde{S}} - \nabla A(\theta))^\top \left(\frac{1}{n} I(\theta) + \sigma^2 I \right)^{-1} (\tilde{\tilde{S}} - \nabla A(\theta)).$$

Numerical stabilization. In finite samples (especially under strong privacy), the estimated Fisher information $I(\tilde{\theta})$ can be ill-conditioned and the noise-aware objective can become flat. In our implementation we apply the following numerical safeguards: (i) Tikhonov regularization $I(\theta) \leftarrow I(\theta) + \lambda I$ with $\lambda = \max(10^{-6}, 0.01 \sigma^2)$; (ii) box constraints $\theta_j \in [-10, 10]$ for the L-BFGS-B optimizer; (iii) a quadratic anchor penalty $0.1 \sigma^2 \sum_j (\theta_j - \hat{\theta}_{\text{plug},j})^2$ in the noise-aware objective; and (iv) clipping of variance diagonal entries at $10^6/n$. These choices are purely for stability and do not change the first-order asymptotic theory.

Proposition 1 (First-order equivalence). *Under Theorem 2’s conditions and with smoothness of $I(\theta)$, the noise-aware estimator $\tilde{\theta}_{\text{NA}}$ is first-order equivalent to the plug-in estimator:*

$$\tilde{\theta}_{\text{NA}} - \tilde{\theta}_{\text{plug}} = o_p(n^{-1/2}) + o_p(\sigma),$$

and thus has the same asymptotic distribution as in Theorem 2.

Proof sketch. At the plug-in solution, $\tilde{\tilde{S}} - \nabla A(\tilde{\theta}_{\text{plug}}) = 0$, which also zeros the noise-aware first-order condition. Hence both estimators solve the same equation at leading order; the difference arises only through higher-order terms involving $\Sigma(\tilde{\theta}_{\text{plug}})^{-1} - \Sigma(\theta_0)^{-1}$, which is $O_p(n^{-1/2} + \sigma)$. See Appendix B for details. \square

4.4 CONFIDENCE INTERVALS AND HYPOTHESIS TESTING

Theorem 2 suggests a Wald interval for each coordinate θ_j :

$$\text{CI}_j = \left[\tilde{\theta}_j \pm z_{1-\alpha/2} \sqrt{\widehat{\text{Var}}(\tilde{\theta})_{jj}} \right],$$

with variance estimate

$$\widehat{\text{Var}}(\tilde{\theta}) = \frac{1}{n} \hat{I}^{-1} + \sigma^2 \hat{I}^{-2}, \quad \hat{I} := I(\tilde{\theta}).$$

where $\widehat{\text{Var}}(\tilde{\theta})_{jj}$ denotes the j -th diagonal entry of $\widehat{\text{Var}}(\tilde{\theta})$. Alternatively, one can use a DP parametric bootstrap to better capture finite-sample effects and clipping bias [Ferrando et al., 2022]. The bootstrap draws are generated from the noise-aware distribution $p(\tilde{\tilde{S}} \mid \theta)$, so the noise-aware likelihood model directly enables the bootstrap procedure; see Appendix D for implementation details.

5 LOWER BOUNDS

Upper bounds are only useful if they are close to optimal. We provide a simple lower bound that matches the *privacy term rate*.

Theorem 3 (Unavoidable $\Omega(1/(n^2\varepsilon^2))$ MSE lower bound). *Consider the one-dimensional exponential family on $\mathcal{X} = \{-1, +1\}$ with $s(x) = x$ and natural parameter $\theta \in \Theta \subset \mathbb{R}$. For any (ε, δ) -DP estimator $\hat{\theta}$ based on n i.i.d. samples with $\delta < 1/4$ and $\varepsilon \in (0, 1]$,*

$$\inf_{\hat{\theta} \text{ } (\varepsilon, \delta)\text{-DP}} \sup_{\theta \in \Theta} \mathbb{E}_\theta \left[(\hat{\theta} - \theta)^2 \right] \geq \frac{c}{n^2 \varepsilon^2},$$

for a universal constant $c > 0$. In particular, the minimax RMSE is at least $\sqrt{c}/(n\varepsilon)$. Combined with Theorem 2, this shows that the $1/(n\varepsilon)$ privacy distortion rate (up to log factors in δ) is minimax optimal in this canonical subclass.

Proof sketch. Write the mean parameter as $\mu(\theta) = \tanh(\theta)$. Given any DP estimator $\hat{\theta}$, the post-processed estimator $\hat{\mu} = \tanh(\hat{\theta})$ is also DP and satisfies $|\hat{\mu} - \mu(\theta)| \leq |\hat{\theta} - \theta|$ since \tanh is 1-Lipschitz. Thus, any minimax lower bound for DP mean estimation transfers immediately to θ . The stated rate follows by specializing the central-model minimax lower bounds for bounded mean estimation under (ε, δ) -DP due to Cai et al. [2021]. See Appendix C for the full argument. \square

6 EXPERIMENTS

The experiments are designed to validate three claims: (i) the asymptotic variance formula in Theorem 2 accurately predicts finite-sample behavior, (ii) Wald confidence intervals achieve nominal coverage, and (iii) plug-in and noise-aware estimators are compared under clipping.

6.1 EXPERIMENTAL DESIGN

All experiments use (ε, δ) -DP with $\delta = 1/n^2$, a standard choice that makes the δ -failure probability negligible relative to the sample.

Models and sufficient statistics. We consider three canonical exponential families.

1. **Gaussian mean estimation.** Data $X_i \sim \mathcal{N}(\mu, \sigma_0^2)$ with known σ_0^2 . Sufficient statistic: $s(x) = x$. Natural parameter: $\theta = \mu/\sigma_0^2$. Clipping: truncate observations to $[-B, B]$.
2. **Logistic regression.** Binary outcomes (X_i, Y_i) with $\Pr(Y = 1 \mid X) = \text{sigmoid}(\theta^\top X)$. Sufficient statistic: $s(x, y) = yx \in \mathbb{R}^d$. Clipping: project features to $\|X\|_2 \leq B$.
3. **Poisson regression.** Count outcomes $Y_i \mid X_i \sim \text{Poisson}(\exp(\theta^\top X_i))$. Sufficient statistic: $s(x, y) = yx$. Clipping: truncate Y to $[0, B_Y]$ and project features to $\|X\|_2 \leq B_X$.

Methods compared.

- **Non-private MLE** (oracle): standard MLE with classical asymptotic CIs.
- **DP plug-in (Wald)**: Algorithm 1 with Wald CIs using the variance formula from Theorem 2.
- **DP noise-aware (Wald)**: the estimator from Section 4.3 with the same CI formula.
- **DP parametric bootstrap**: the bootstrap procedure of Ferrando et al. [2022] adapted to sufficient-statistic release, where bootstrap samples are drawn from the noisy statistic’s distribution.
- **Naive DP synthetic**: generate $D^{\text{syn}} \sim p(\cdot \mid \tilde{\theta}_{\text{plug}})$, then apply standard (non-DP-aware) MLE and CIs to D^{syn} .

Metrics.

- **Coverage**: empirical coverage of nominal 95% confidence intervals across 1000 independent runs (each with fresh data and DP noise).
- **Interval length**: average CI width, measuring inferential precision.
- **Parameter MSE**: $\mathbb{E}[\|\tilde{\theta} - \theta_0\|^2]$, estimated over replications.
- **Type-I error**: rejection rate of $H_0 : \theta_j = \theta_{0,j}$ at the true parameter.
- **Power**: rejection rate at a sequence of alternatives $\theta_j = \theta_{0,j} + \Delta$ for $\Delta \in \{0.1, 0.2, 0.5, 1.0\}$.

6.2 SIMULATION EXPERIMENTS

Experiment 1: variance inflation validation. For the Gaussian model with $d = 1$, compute the empirical variance of $\tilde{\theta}_{\text{plug}}$ across 5000 replications and compare to the theoretical prediction $I(\theta_0)^{-1}/n + \sigma^2 I(\theta_0)^{-2}$. Vary $n \in \{100, 500, 1000, 5000\}$ and $\varepsilon \in \{0.1, 0.5, 1.0, 5.0, 10.0\}$. Plot empirical vs. theoretical variance as a scatter plot; points should lie on the diagonal.

Experiment 2: coverage across the privacy spectrum. For each model and each (ε, n) pair, compute 95% Wald CIs using both plug-in and noise-aware estimators. Report coverage as a function of ε for fixed n (and vice versa). The key prediction is that coverage should be near-nominal for all methods when $n\varepsilon^2 \gg 1$, but naive synthetic data analysis should have severely undercovered intervals especially when ε is small.

Experiment 3: plug-in vs. noise-aware under clipping. For logistic regression with $d = 5$, vary the clipping radius B from aggressive ($B = 1$) to generous ($B = 10$) and measure bias and coverage. We test whether the noise-aware estimator shows less bias and better coverage when B is small relative to the natural data scale.

Experiment 4: scaling law validation. For the Gaussian model, plot MSE vs. n on a log-log scale for several values of ε . The theoretical prediction is $\text{MSE} \approx c_1/n + c_2/(n^2\varepsilon^2)$, which should appear as two distinct slopes on the log-log plot. Identify the crossover point where the privacy term begins to dominate.

6.3 REAL DATA EXPERIMENTS

Dataset. We use the American Community Survey (ACS) Public Use Microdata Sample, following the Folktables framework [Ding et al., 2021] which provides standardized prediction tasks. Specifically, we consider the ACSIncome task (predicting whether income exceeds \$50,000) for California, 2018. After dropping rows with missing values, we standardize all features to zero mean and unit variance, then select the $d = 10$ covariates with highest marginal variance, yielding a logistic regression problem. Features are clipped to $\|X\|_2 \leq B$ with $B = 3.0$ (post-standardization), giving ℓ_2 sensitivity $\Delta_2 = 2B/n = 6/n$. The large full sample ($n \approx 1.6\text{M}$) allows us to treat the full-data MLE as the ground truth θ_0 .

Protocol. Subsample datasets of size $n \in \{500, 1000, 5000, 10000\}$ and apply our pipeline at $\varepsilon \in \{0.5, 1.0, 2.0, 5.0\}$. For each configuration, run 500 replications. Report coverage and interval length of Wald CIs for each regression coefficient, averaged across coordinates.

6.4 SYNTHETIC DATA EVALUATION

Generate parametric synthetic data D^{syn} from $\tilde{\theta}$ and evaluate:

- Whether point estimates and CIs computed on D^{syn} (with noise-aware correction) match those from the DP statistic release. Since both are post-processing of the same \tilde{S} , the estimators should agree, but the CI widths may differ depending on n_{syn} .
- How naive analysis (treating D^{syn} as real data) miscalibrates uncertainty, replicating and extending the findings of Räisä et al. [2023], Perez et al. [2024]. We expect severe undercoverage, especially for small ε .
- The effect of synthetic sample size n_{syn} on Monte Carlo error, verifying that $n_{\text{syn}} \gg n$ is needed to make the synthetic sampling error negligible.

6.5 RESULTS

Experiment 1: variance inflation validation. Figure 2 compares the empirical variance of the DP plug-in estimator to the theoretical prediction from Theorem 2, namely $I(\theta_0)^{-1}/n + \sigma^2 I(\theta_0)^{-2}$. In the Gaussian model ($d = 1$), this reduces to $1/n + \sigma^2$, so each point corresponds to one (n, ε) pair and should lie on the identity line if the finite-sample behavior matches the asymptotic formula.

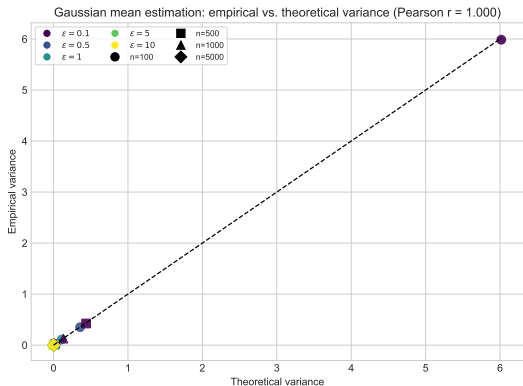


Figure 2: Empirical versus theoretical variance for the DP plug-in estimator in Gaussian mean estimation. Each point corresponds to one (n, ϵ) configuration, with color indicating ϵ and marker shape indicating n . The close alignment with the identity line validates the finite-sample relevance of Theorem 2.

The points concentrate tightly around the diagonal across all privacy levels and sample sizes, with near-perfect linear agreement. The Pearson correlation between theoretical and empirical variance is $r = 0.9999978$, and the maximum relative error across the 20 (n, ϵ) settings is 3.67%. This confirms that the additive decomposition into sampling noise and privacy noise is already accurate in finite samples, supporting the practical use of our Wald variance formula without extra calibration.

Experiment 2: coverage across the privacy spectrum. Figure 3 reports 95% coverage as a function of ϵ for Gaussian, logistic, and Poisson models at two sample sizes. Across all models and (n, ϵ) combinations, non-private coverage stays in $[0.941, 0.961]$, DP plug-in Wald in $[0.768, 1.000]$, DP noise-aware Wald in $[0.768, 1.000]$, and DP bootstrap in $[0.765, 1.000]$. The worst calibrated private setting for these three methods is the Poisson model at $(n, \epsilon) = (500, 0.1)$, where coverage is approximately 0.77.

The naive synthetic-data baseline severely undercovers, ranging from 0.014 to 0.844, with minimum coverage at Poisson $(n, \epsilon) = (500, 0.1)$. At $\epsilon = 0.1$, its mean coverage across all models and n is only 0.079. Thus Figure 3 and Table 1 both show that accounting for privacy noise is essential for valid uncertainty quantification.

The Poisson model shows the worst calibration among the three families (coverage ≈ 0.77 at $n=500, \epsilon=0.1$), reflecting a finite-sample Wald breakdown: for log-link models, $I(\theta) = X^T \text{diag}(\exp(X\theta)) X/n$ depends on θ through the convex $\exp(\cdot)$, so by Jensen’s inequality $I(\tilde{\theta})$ is systematically inflated when privacy noise is large, yielding CIs that are too narrow. This effect vanishes as ϵ grows. Poisson coverage is further hampered by the high sensitivity of $s(x, y) = yx$: with $B_X = 3, B_Y = 20$, the effective bound is $B = 60$, producing large noise at strong privacy.

Table 1: Summary: 95% CI Coverage across Methods and Privacy Levels (Gaussian Model, $n = 1000$).

| Method | $\epsilon=0.1$ | $\epsilon=0.5$ | $\epsilon=1.0$ | $\epsilon=5.0$ | $\epsilon=10$ |
|---------------------|----------------|----------------|----------------|----------------|---------------|
| Non-private MLE | 0.947 | 0.958 | 0.954 | 0.948 | 0.948 |
| DP plug-in Wald | 0.950 | 0.947 | 0.951 | 0.950 | 0.955 |
| DP noise-aware Wald | 0.950 | 0.947 | 0.951 | 0.950 | 0.955 |
| DP param. bootstrap | 0.944 | 0.945 | 0.945 | 0.945 | 0.948 |
| Naive DP synthetic | 0.146 | 0.499 | 0.679 | 0.848 | 0.831 |

Experiment 2 (precision trade-off): CI lengths. Figure 4 complements the coverage plot by reporting average CI length. At small ϵ , valid DP methods widen intervals to absorb privacy uncertainty, while naive synthetic analysis remains artificially narrow. This pattern explains the simultaneous undercoverage and apparent precision of the naive baseline.

As ϵ grows, interval lengths for DP-aware methods contract toward the non-private benchmark, matching the asymptotic efficiency transition predicted by Corollary 1. Together, Figures 3 and 4 demonstrate that honest calibration requires wider intervals precisely where privacy noise is strongest.

Experiment 3: plug-in versus noise-aware under clipping. Figure 5 isolates clipping effects in logistic regression by varying the clipping radius B while fixing $(n, \epsilon) = (1000, 1.0)$.

The results reveal a U-shaped bias curve reflecting the sensitivity–accuracy tradeoff. At aggressive clipping ($B \leq 1.0$), clipping bias dominates: at $B = 0.5$, plug-in has absolute bias 2.323 and coverage 0.116, while noise-aware has bias 2.767 and coverage 0.088. At moderate clipping ($B = 2.0\text{--}3.0$), both methods reduce bias to 0.16–0.29 and improve coverage to 0.81–0.98. At generous clipping ($B = 5.0\text{--}10.0$), clipping bias vanishes but $\sigma \propto 2B/n$ grows linearly with B , increasing error (bias 0.24–1.06); coverage remains good (0.96–0.97) because Wald intervals correctly widen.

The noise-aware estimator does not outperform plug-in in any setting, consistent with Proposition 1: the second-order correction does not help and may hurt when the CLT approximation to clipped data is poor. These results suggest choosing B at 2–3 standard deviations of the features, balancing clipping bias against sensitivity-driven noise.

Experiment 4: scaling law validation. Figure 6 shows log-log MSE curves for multiple ϵ values against sample size n . The empirical curves follow the theoretical form $c_1/n + c_2/(n^2\epsilon^2)$, with a privacy-dominated regime at smaller n and a sampling-dominated regime at larger n . The first grid point where privacy variance is no larger than sampling variance is $n = 100$ for $\epsilon = 5$, $n = 500$ for $\epsilon = 2$, $n = 5,000$ for $\epsilon = 1$, and $n = 10,000$ for $\epsilon = 0.5$. At large n , all DP curves approach the non-private $1/n$ baseline, confirming that privacy overhead vanishes asymptotically. The crossover ordering matches theory: larger ϵ shifts the

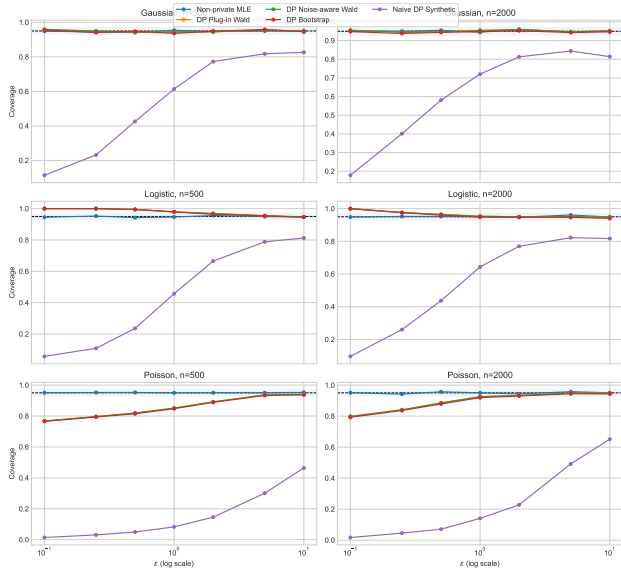


Figure 3: Coverage of 95% intervals across privacy levels for Gaussian, logistic, and Poisson models, each at two sample sizes. The shaded band marks an acceptable calibration range around nominal coverage. Noise-calibrated DP methods remain near nominal while naive synthetic analysis undercovers in the low- ϵ regime.

transition to smaller n , consistent with both Theorem 2 and Theorem 3.

Experiment 5: type-I error and power. Figure 7 reports rejection rates for Wald tests across alternatives Δ and privacy levels. At $\Delta = 0$ and $\epsilon = 1.0$, type-I error is 0.0385 for DP plug-in/noise-aware, 0.0515 for non-private, and 0.292 for naive synthetic. Across privacy levels, naive synthetic remains anti-conservative under the null (type-I error from 0.488 at $\epsilon = 0.5$ to 0.184 at $\epsilon = 5.0$).

As Δ increases, all methods gain power; for example at $\epsilon = 1.0$ and $\Delta = 0.1$, DP power is 0.481 versus 0.873 non-private. By $\Delta = 0.2$, DP power reaches 0.967 and non-private reaches 1.000. The expected privacy-power trade-off is visible at lower ϵ , where calibrated methods pay power to maintain valid size. Thus, proper noise calibration delivers valid tests while preserving competitive sensitivity to true effects.

Experiment 6: real data (ACS/Folktables). Figure 8 summarizes ACSIncome logistic-regression results over (n, ϵ) grids using the full-data MLE as ground truth. Across all (n, ϵ) settings, mean coverage is 0.889 for DP plug-in, 0.888 for DP noise-aware, 0.880 for DP bootstrap, and 0.510 for naive synthetic. The naive method is worst at $(n, \epsilon) = (500, 0.5)$ with coverage 0.134, while the private calibrated methods at that setting are all near 1.0.

After the numerical stabilization in Section 4.3, CI lengths remain finite in all settings: for DP plug-in they range from 0.127 to 90.835, for DP noise-aware from 0.127 to 93.912, and for DP bootstrap from 0.125 to 137.185. Naive synthetic intervals are much shorter (0.118 to 2.735) but

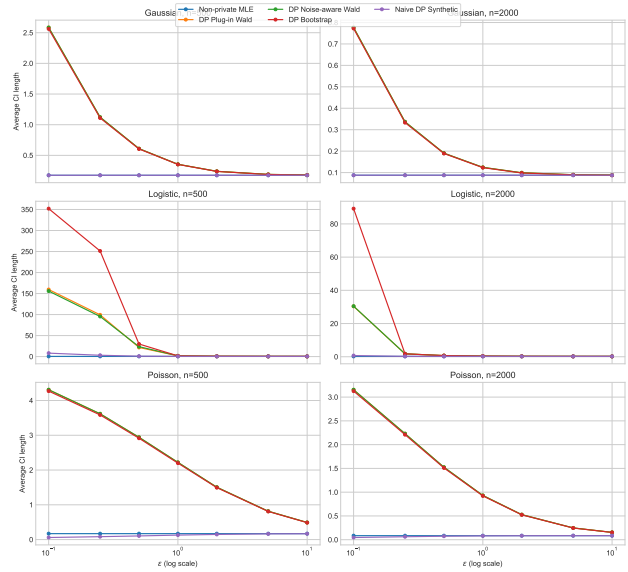


Figure 4: Average confidence-interval length versus ϵ for the same settings as Figure 3. Noise-aware methods are wider at strong privacy (small ϵ) and contract as ϵ increases, reflecting the expected privacy-accuracy trade-off. Naive synthetic intervals remain narrow but are miscalibrated.

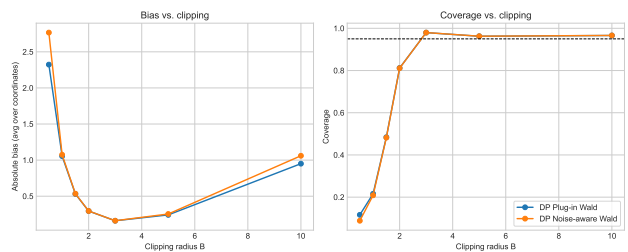


Figure 5: Logistic-regression clipping study comparing DP plug-in and DP noise-aware estimators. Left: average absolute bias versus clipping radius B . Right: empirical 95% coverage versus B . Both methods exhibit a U-shaped bias curve: too-small B causes clipping bias while too-large B increases noise through higher sensitivity. The noise-aware estimator provides no advantage over plug-in, consistent with Proposition 1.

substantially undercovered. These results indicate that the sufficient-statistic release pipeline is practical beyond idealized synthetic settings.

Experiment 7: synthetic-data inferential evaluation. Figure 9 compares three analysis modes as synthetic sample size n_{syn} grows. Direct inference from $\hat{\theta}$ has coverage 0.952 at all ratios, while noise-aware synthetic analysis is 0.942, 0.943, 0.954, 0.957 for $n_{\text{syn}}/n = 1, 5, 10, 50$. Naive synthetic analysis is severely undercovered at every ratio: 0.685, 0.391, 0.282, 0.136.

Increasing n_{syn} reduces only synthetic Monte Carlo noise, not the privacy distortion inherited from $\tilde{\theta}$. Thus synthetic sample size alone cannot fix inferential miscalibration caused by ignoring privacy noise.

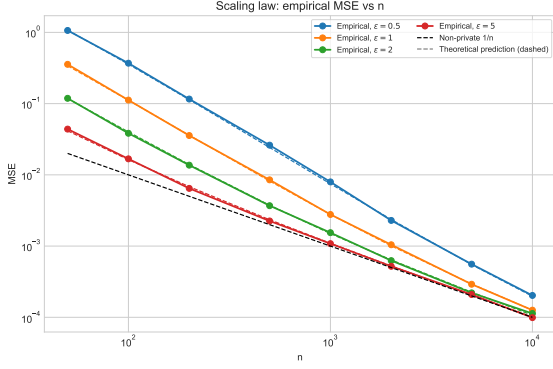


Figure 6: Log-log MSE scaling for Gaussian mean estimation. Solid lines are empirical MSE for each ϵ ; dashed color-matched lines are theoretical predictions; the thin black dashed line is non-private $1/n$. The observed two-regime behavior matches the predicted $1/n + 1/(n^2 \epsilon^2)$ structure.

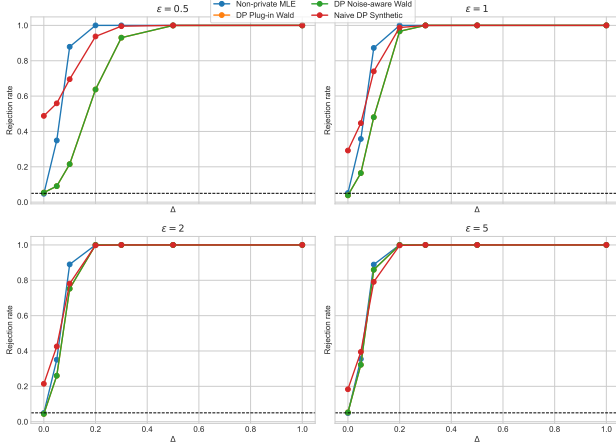


Figure 7: Power curves and type-I error diagnostics for Gaussian Wald tests across four privacy levels. At $\Delta = 0$, calibrated DP methods remain near the nominal 0.05 level while naive synthetic testing is inflated. Power increases with effect size and approaches non-private behavior as ϵ grows.

7 DISCUSSION AND EXTENSIONS

Experimental takeaways. Across all experiments, the variance inflation formula from Theorem 2 is highly accurate, calibrated DP inference strongly outperforms naive synthetic-data analysis, and plug-in and noise-aware estimators behave similarly outside extreme finite-sample regimes, consistent with Proposition 1.

Beyond exponential families. The sufficient-statistic release idea extends to M-estimation and the generalized method of moments, where “sufficient statistics” become empirical moment conditions $n^{-1} \sum_i \psi(X_i; \theta)$ that can be privatized and used for noise-aware inference, connecting naturally to workload-based synthesis and causal inference pipelines.

Noise shaping and matrix mechanisms. For high-dimensional d , isotropic Gaussian noise may be suboptimal. Matrix mechanisms [Li et al., 2015] can reduce variance



Figure 8: Real-data ACSIncome evaluation across (n, ϵ) configurations. The top panel reports average coefficient coverage and the bottom panel reports average CI length. DP plug-in and noise-aware methods maintain substantially better calibration than naive synthetic analysis, with the largest gains in low- n , low- ϵ settings.

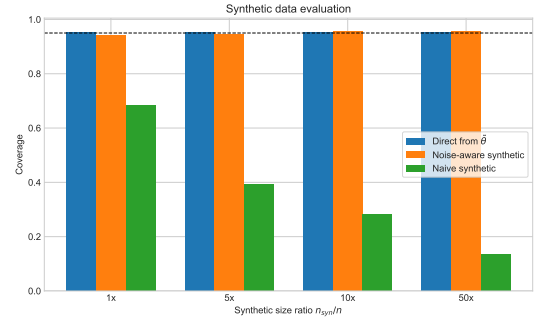


Figure 9: Coverage comparison for direct DP inference, noise-aware synthetic analysis, and naive synthetic analysis across synthetic sample-size ratios. Direct and noise-aware approaches remain near nominal coverage, while naive analysis systematically undercovers. Larger synthetic datasets do not eliminate the need for privacy-aware uncertainty correction.

in target directions by releasing a linear transform $M\bar{S}$ with noise calibrated to the sensitivity of $M\bar{S}$; extending our theory to this setting is straightforward, requiring only a modified sensitivity analysis for the transformed query $M\bar{S}$.

Composition with DP-SGD. When B is unknown a priori and data-dependent clipping is used (as in differentially private stochastic gradient descent, DP-SGD), the sensitivity analysis becomes more involved; investigating this interaction is an important practical direction.

Multivariate confidence regions. Our Wald intervals are coordinate-wise; simultaneous ellipsoidal regions can be constructed from the same variance formula and are left for future work.

Limitations. Our pipeline requires a regular exponential family with known sufficient statistics; extending to semi-parametric or nonparametric models needs different tools. Wald CIs can undercover at low ϵ for convex-link models (e.g., Poisson) due to Jensen’s inequality inflating $I(\hat{\theta})$; bootstrap CIs may help. The clipping radius B trades off clipping bias against noise magnitude, closely related to bias–accuracy–privacy trilemmas [Kamath et al., 2025].

Acknowledgements

References

- Daniel Alabi and Salil Vadhan. Hypothesis testing for differentially private linear regression. In *Advances in Neural Information Processing Systems*, 2022.
- Marco Avella-Medina, James Bradshaw, and Po-Ling Loh. Differentially private inference via noisy optimization. *The Annals of Statistics*, 51(5), 2023. doi: 10.1214/23-AOS2321.
- Jordan Awan and Aleksandra Slavković. Differentially private uniformly most powerful tests for binomial data. In *Advances in Neural Information Processing Systems*, volume 31, 2018.
- Jordan Awan and Yuguang Wang. Simulation-based, finite-sample inference for privatized data. *Journal of the American Statistical Association*, 120(551):1669–1682, 2025. doi: 10.1080/01621459.2024.2427436.
- Borja Balle and Yu-Xiang Wang. Improving the Gaussian mechanism for differential privacy: Analytical calibration and optimal denoising. In *Proceedings of the 35th International Conference on Machine Learning (ICML)*, volume 80 of *Proceedings of Machine Learning Research*, pages 403–412. PMLR, 2018.
- Garrett Bernstein and Daniel Sheldon. Differentially private bayesian inference for exponential families. In *Advances in Neural Information Processing Systems*, volume 31, pages 2924–2934, 2018.
- T. Tony Cai, Yichen Wang, and Linjun Zhang. The cost of privacy: Optimal rates of convergence for parameter estimation with differential privacy. *Annals of Statistics*, 49(5):2825–2850, 2021.
- Christian Covington, Xi He, James Honaker, and Gautam Kamath. Unbiased statistical estimation and valid confidence intervals under differential privacy. *Statistica Sinica*, 35:651–670, 2025.
- Frances Ding, Moritz Hardt, John Miller, and Ludwig Schmidt. Retiring adult: New datasets for fair machine learning. In *Advances in Neural Information Processing Systems*, volume 34, pages 6478–6490, 2021.
- Jinshuo Dong, Aaron Roth, and Weijie J. Su. Gaussian differential privacy. *Journal of the Royal Statistical Society Series B: Statistical Methodology*, 84(1):3–37, 2022. doi: 10.1111/rssb.12454.
- Konstantin Donhauser, Javier Abad, Neha Hulkund, and Fanny Yang. Privacy-preserving data release leveraging optimal transport and particle gradient descent. In *Proceedings of the 41st International Conference on Machine Learning (ICML)*, 2024.
- John C. Duchi, Michael I. Jordan, and Martin J. Wainwright. Minimax optimal procedures for locally private estimation. *Journal of the American Statistical Association*, 113(521):182–201, 2018.
- Cynthia Dwork and Aaron Roth. *The Algorithmic Foundations of Differential Privacy*, volume 9 of *Foundations and Trends in Theoretical Computer Science*. Now Publishers, 2014.
- Cynthia Dwork, Frank McSherry, Kobbi Nissim, and Adam Smith. Calibrating noise to sensitivity in private data analysis. In *Theory of Cryptography Conference (TCC)*, pages 265–284. Springer, 2006.
- Cecilia Ferrando, Shufan Wang, and Daniel Sheldon. Parametric bootstrap for differentially private confidence intervals. In *Proceedings of The 25th International Conference on Artificial Intelligence and Statistics (AISTATS)*, volume 151 of *Proceedings of Machine Learning Research*, pages 1598–1618. PMLR, 2022.
- Gautam Kamath, Argyris Mouzakis, Matthew Regehr, and Vatsal Singhal. A bias-accuracy-privacy trilemma for statistical estimation. *Journal of the American Statistical Association*, 120(552):2338–2349, 2025. doi: 10.1080/01621459.2024.2443275.
- Vishesh Karwa and Aleksandra Slavković. Inference using noisy degrees: Differentially private β -model and synthetic graphs. *The Annals of Statistics*, 44(1), 2016. doi: 10.1214/15-AOS1358.
- Vishesh Karwa and Salil P. Vadhan. Finite sample differentially private confidence intervals. In *9th Innovations in Theoretical Computer Science Conference (ITCS)*, volume 94 of *LIPICs*, pages 44:1–44:9. Schloss Dagstuhl - Leibniz-Zentrum für Informatik, 2018. doi: 10.4230/LIPICs.ITCS.2018.44.
- Chao Li, Gerome Miklau, Michael Hay, Andrew McGregor, and Vibhor Rastogi. The matrix mechanism: Optimizing linear counting queries under differential privacy. *The VLDB Journal*, 24(6):757–781, 2015.
- Ryan McKenna, Gerome Miklau, and Daniel Sheldon. Winning the NIST contest: A scalable and general approach to differentially private synthetic data. *Journal of Privacy and Confidentiality*, 11(3), 2021.
- Ryan McKenna, Brett Mullins, Daniel Sheldon, and Gerome Miklau. AIM: An adaptive and iterative mechanism for differentially private synthetic data. *Proceedings of the VLDB Endowment*, 15(11):2599–2612, 2022. doi: 10.14778/3551793.3551817.
- Ileana Montoya Perez, Parisa Movahedi, Valtteri Niemi, Antti Airola, and Tapio Pahikkala. Does differentially private synthetic data lead to synthetic discover-

ies? *Methods of Information in Medicine*, 2024. doi: 10.1055/a-2385-1355. Published online Sep 9, 2024.

Ossi Räisä, Joonas Jälkö, Samuel Kaski, and Antti Honkela. Noise-aware statistical inference with differentially private synthetic data. In *Proceedings of The 26th International Conference on Artificial Intelligence and Statistics (AISTATS)*, volume 206 of *Proceedings of Machine Learning Research*, pages 3620–3643. PMLR, 2023.

Adam Smith. Privacy-preserving statistical estimation with optimal convergence rates. In *Proceedings of the 43rd Annual ACM Symposium on Theory of Computing (STOC)*, pages 813–821. ACM, 2011.

Yuchao Tao, Ryan McKenna, Michael Hay, Ashwin Machanavajjhala, and Gerome Miklau. Benchmarking differentially private synthetic data generation algorithms. *arXiv preprint arXiv:2112.09238*, 2022.

Zhanyu Wang, Guang Cheng, and Jordan Awan. Differentially private bootstrap: New privacy analysis and inference strategies. *Journal of Machine Learning Research*, 26:1–57, 2025.

Larry Wasserman and Shuheng Zhou. A statistical framework for differential privacy. *Journal of the American Statistical Association*, 105(489):375–389, 2010. doi: 10.1198/jasa.2009.tm08651.

Noise-Calibrated Inference from Differentially Private Sufficient Statistics in Exponential Families (Supplementary Material)

Amir Asiaee¹

Samhita Pal¹

¹Department of Biostatistics, Vanderbilt University Medical Center, Nashville, TN, USA
{amir.asiaee, samhita.pal}@vumc.org

A PROOF OF THEOREM 2 (ASYMPTOTIC DISTRIBUTION AND VARIANCE INFLATION)

Proof. Recall that $\mu(\theta) := \nabla A(\theta) = \mathbb{E}_\theta[s(X)]$ is the mean parameter map, and $(\nabla A)^{-1}$ is its inverse. We decompose:

$$\tilde{\theta}_{\text{plug}} - \theta_0 = (\nabla A)^{-1}(\tilde{S}) - \theta_0 = (\nabla A)^{-1}(\bar{S} + Z) - \theta_0.$$

Step 1 (sampling term). By the law of large numbers, $\bar{S} \xrightarrow{p} \mu(\theta_0)$. By the multivariate CLT applied to $s(X_1), \dots, s(X_n)$,

$$\sqrt{n}(\bar{S} - \mu(\theta_0)) \xrightarrow{d} \mathcal{N}(0, \text{Cov}_{\theta_0}[s(X)]) = \mathcal{N}(0, I(\theta_0)),$$

where the last equality uses the identity $\text{Cov}_{\theta_0}[s(X)] = \nabla^2 A(\theta_0) = I(\theta_0)$ for minimal exponential families. Since $(\nabla A)^{-1}$ is differentiable at $\mu(\theta_0)$ with Jacobian $I(\theta_0)^{-1}$, the delta method gives $\sqrt{n}(\hat{\theta} - \theta_0) \xrightarrow{d} \mathcal{N}(0, I(\theta_0)^{-1})$.

Step 2 (privacy term). By a first-order Taylor expansion of $(\nabla A)^{-1}$ around \bar{S} ,

$$\tilde{\theta}_{\text{plug}} - \hat{\theta} = (\nabla A)^{-1}(\bar{S} + Z) - (\nabla A)^{-1}(\bar{S}) = I(\hat{\theta})^{-1}Z + O_p(\|Z\|^2).$$

Since $Z \sim \mathcal{N}(0, \sigma^2 I_d)$, we have $\|Z\| = O_p(\sigma)$ and thus the remainder term is $O_p(\sigma^2) = o_p(\sigma)$. Because $I(\hat{\theta}) \xrightarrow{p} I(\theta_0)$, we have $\tilde{\theta}_{\text{plug}} - \hat{\theta} = I(\theta_0)^{-1}Z + o_p(\sigma)$.

Step 3 (combining). The sampling term $\hat{\theta} - \theta_0$ depends only on $\{X_i\}$, while Z is independent of the data. Therefore the covariance of the two terms is zero, and

$$\sqrt{n}(\tilde{\theta}_{\text{plug}} - \theta_0) \xrightarrow{d} \mathcal{N}\left(0, I(\theta_0)^{-1} + n\sigma^2 I(\theta_0)^{-2}\right).$$

The rate decomposition follows from the fact that, under Gaussian-mechanism calibration, σ is proportional to the sensitivity $\Delta_2 = 2B/n$ (up to $\log(1/\delta)$ factors), yielding the $O_p((n\varepsilon)^{-1})$ privacy distortion rate for bounded problems. \square

B PROOF OF PROPOSITION 1 (FIRST-ORDER EQUIVALENCE)

Proof. The plug-in estimator solves $\nabla A(\theta) = \tilde{S}$, while the noise-aware estimator minimizes the weighted quadratic $Q(\theta) = (\tilde{S} - \nabla A(\theta))^\top \Sigma(\theta)^{-1}(\tilde{S} - \nabla A(\theta))$ with $\Sigma(\theta) = I(\theta)/n + \sigma^2 I$. The noise-aware first-order condition is $\nabla A(\theta)^\top [\nabla^2 A(\theta)] \Sigma(\theta)^{-1}(\tilde{S} - \nabla A(\theta)) = 0$. At the plug-in solution, $\tilde{S} - \nabla A(\tilde{\theta}_{\text{plug}}) = 0$, which also sets this expression to zero. Hence both estimators solve the same equation at leading order.

More precisely, expand $Q(\theta)$ around $\tilde{\theta}_{\text{plug}}$. The difference $\tilde{\theta}_{\text{NA}} - \tilde{\theta}_{\text{plug}}$ satisfies a Newton-type update whose magnitude is controlled by $\left\| \Sigma(\tilde{\theta}_{\text{plug}})^{-1} - \Sigma(\theta_0)^{-1} \right\| = O_p(n^{-1/2} + \sigma)$ times lower-order terms. By standard M-estimation arguments, this yields $\tilde{\theta}_{\text{NA}} - \tilde{\theta}_{\text{plug}} = o_p(n^{-1/2}) + o_p(\sigma)$. \square

C PROOF OF THEOREM 3 (LOWER BOUND)

Proof. Let $X \in \{-1, +1\}$ and write the mean parameter as $\mu(\theta) = \mathbb{E}_\theta[X] = \tanh(\theta)$. Let $\hat{\theta}$ be any (ε, δ) -DP estimator of θ based on n i.i.d. samples and define the post-processed mean estimator $\hat{\mu} := \tanh(\hat{\theta})$. By post-processing invariance, $\hat{\mu}$ is also (ε, δ) -DP. Since \tanh is 1-Lipschitz, we have the pointwise inequality $(\hat{\mu} - \mu(\theta))^2 \leq (\hat{\theta} - \theta)^2$ and therefore

$$\mathbb{E}_\theta \left[(\hat{\theta} - \theta)^2 \right] \geq \mathbb{E}_\theta \left[(\hat{\mu} - \mu(\theta))^2 \right].$$

It therefore suffices to lower bound the minimax mean-estimation risk under central (ε, δ) -DP. The minimax lower bounds of Cai et al. [2021] for bounded mean estimation imply that, for $\varepsilon \in (0, 1]$ and $\delta < 1/4$,

$$\inf_{\hat{\mu} \text{ } (\varepsilon, \delta)\text{-DP}} \sup_{\mu \in [-1, 1]} \mathbb{E}[(\hat{\mu} - \mu)^2] \geq \frac{c}{n^2 \varepsilon^2}$$

for a universal constant $c > 0$. Applying this bound to our Bernoulli family and combining with the inequality above yields the stated lower bound for θ . \square

D ADDITIONAL EXPERIMENTAL DETAILS

Replication counts. All simulation experiments use sufficient replications for stable Monte Carlo estimates: Experiment 1 uses 5,000 replications, Experiments 2–3 use 1,000, Experiments 4–5 use 2,000, Experiment 6 (real data) uses 500, and Experiment 7 uses 1,000. The DP parametric bootstrap uses $B_{\text{boot}} = 500$ draws in simulation experiments and $B_{\text{boot}} = 200$ in the real-data experiment.

Runtime. On a single machine with 8 CPU cores, the full experiment suite (Experiments 1–7 with all models and configurations) runs in approximately 4–6 hours. Individual experiments range from 2 minutes (Experiment 1, Gaussian only) to 90 minutes (Experiment 6, real data with 500 replications across 16 (n, ε) configurations). The noise-aware estimator adds negligible overhead compared to plug-in, since both require a single optimization step per replication.

Software. All experiments are implemented in Python using NumPy and SciPy. The ACS data in Experiment 6 are accessed via the Folktables package [Ding et al., 2021].